

Buckling Analysis of FG Timoshenko Beam Based on Physical Neutral Surface Position

Pınar Aydan DEMİRHAN^{1*}

¹Trakya University, Faculty of Engineering, Mechanical Engineering Department, Edirne, Türkiye
(ORCID: [0000-0002-2618-4982](https://orcid.org/0000-0002-2618-4982))



Keywords: Buckling analysis, Physical neutral surface position, Critical load, Functionally graded materials, Ritz method, Timoshenko beam.

Abstract

The paper investigates the buckling analysis of the functionally graded Timoshenko beams with arbitrary boundary conditions. The investigation focuses on the critical buckling loads, considering factors such as the slenderness ratio, boundary conditions, and the power-law index. The method involves defining the effective properties of the FG beam by rule of mixture, with physical neutral surface is assumed as a reference surface. Numerical results are presented, demonstrating the variation of the non-dimensional neutral surface position with the power law index for different material property ratios. The study concludes by discussing the influence of slenderness ratio, power law index value, and boundary conditions on critical buckling load of FG Timoshenko beams.

1. Introduction

In recent years, researchers have been focusing on composite materials as conventional materials are unable to meet the demands of high-end technological applications. Although laminated composites are used in a wide range of industrial applications, they have certain limitations due to stress concentrations occurring at their layer interfaces. However, functionally graded (FG) materials overcome these limitations by smoothly varying their properties. This is achieved by the smooth variation of material properties through the thickness direction to attain the desired function. These graded materials are ideal for various applications such as shells, plates, and beams, due to their advantageous features which eliminate sudden changes in properties.

The analysis of functionally graded sandwich plates is essential due to their wide use in aerospace, civil, and mechanical engineering. These plates, which have customized material properties, offer improved performance, including better strength-to-weight ratios and superior resistance to thermal and mechanical loads. Despite significant progress in understanding their behavior, there is still a need for further comprehensive studies to develop more

accurate and efficient models for predicting their responses. This study aims to address these gaps by providing an in-depth analysis of functionally graded sandwich plates using advanced theoretical and computational approaches.

Several studies have presented about the dynamic and the static behavior of the FG beams and plates. Zenkour[1] provided a comprehensive analysis of these plates, Li et al.[2] conducted a three-dimensional vibration analysis. Reddy [3] offered significant insights into the analysis of functionally graded plates. Vo et al.[4] developed a quasi-3D theory for vibration and buckling, and Thai and Choi[5] formulated a finite element approach for various shear deformation theories. Taskin and Demirhan [6] focused on the static analysis of simply supported porous sandwich plates. Demirhan and Taskin[7] investigated bending and free vibration using the state space approach. Vo et al. [8] developed a refined shear deformation theory for the finite element modeling of vibration and buckling. Nair and Pany [9] presented a comprehensive review on the static, buckling, and free vibration, thermo-mechanical analysis of FGM panel. Pany and Rao

*Corresponding author: pinard@trakya.edu.tr

Received: 17.04.2024, Accepted: 03.07.2024

presented studies on the fundamental frequency of a uniform cantilever beam undergoing large amplitude [10] and large amplitude fundamental frequency for a spring-hinged uniform beam [11]. Pany [12] presented a study to provide the large-amplitude first mode frequency for the non-prismatic (tapered beam) cantilever beam. Li and Batra [13] conducted a study on the critical buckling loads of FG Euler-Bernoulli and Timoshenko beams. Li et al. [14], [15] obtained analytical relations of the bending analysis of homogenous Euler-Bernoulli beams and FG Timoshenko beams. An analytical solution is developed by Nguyen et al. [16] for buckling, bending, and vibration of the functionally graded beam (FGB) utilizing the first-order shear deformation beam theory (FOSDT). Li et al. [17] compared functionally graded Levinson and Euler-Bernoulli beams in terms of the critical buckling loads.

Various theories have been used for analyzing functionally graded materials. Anisotropy of the material properties causes complexity for the solution; therefore, researchers investigate the new theories. Morimoto et al. [18] offered a suitably selected reference plane to eliminate coupled bending and stretching deformations. Abrate [19] indicated that choosing an appropriate reference plane enables in-plane and transverse deformations to be uncoupled. Zhang and Zhou [20] called this reference plane to the physical neutral surface (PNS) and emphasized that the stretching and bending deformations are uncoupled in constitutive equations of their theory. They presented a static and dynamic analysis of functionally graded thin plates based on the PNS. Since the calculation procedure of this theory is simpler than the other geometrical middle surface-based theories, it has been used by many researchers.

Concerning functionally graded plates, many research have conducted for static and dynamic analysis. Zhang [21] used PNS concept with high order shear deformation theory for investigation of nonlinear analysis of functionally graded plate (FGP). Fekrar et al. [22] developed a high order shear deformation plate theory for bending analysis of FGP, and used PNS to simplify the solution procedure. Zhang [23] presented a model for FGP resting on two-parameter elastic foundation based on PNS concept with high order shear deformation theory (HOSDT). Han et al. [24] contributed the dynamic instability analysis of Sigmoid FGP on elastic medium, used a four-variable refined plate theory with PNS concept. By utilizing neutral surface position, Bellifa et al. [25] proposed a novel FOSDT for functionally graded plate bending and dynamic analysis. Ebrahimi et al.

[26] investigated the analytical solution for free vibration of shear deformable porous smart plates considering neutral surface position. The four-variable refined theory with PNS concept was used by Nguyen et al. [27] to evaluate the static behavior of FGP resting on Winkler-Pasternak elastic foundation. For analyzing free vibration and mechanical buckling of FGP, Sadgui and Tati [28] established a novel HOSDT based on the precise neutral surface location.

There are limited number of papers dealing with dynamic and static analysis of FG beam using PNS position concept. Ma and Lee [29] offered an exact, closed-form solution for the nonlinear bending and thermal post buckling analysis of FG beam subjected to a uniform in-plane thermal loading using PNS concept. Larbi et al. [30] proposed an efficient beam theory considering shear deformation based on PNS position for free vibration and bending analysis of FGB. Zhang [31] investigated nonlinear vibration and the thermal post-buckling analysis of FGBs using HOSDT with PNS concept. Al-Basyouni et al. [32] presented a modified couple stress theory with neutral axis concept for vibration and bending analysis of FG micro-beams. Ebrahimi and Salari [33] developed a semi-analytical solution for free vibration and buckling of nano-FGBs based on the PNS position. Zoubida et al. [34] conducted the static and free vibration analysis of FGB using a new refined beam theory based on PNS position. Phuong et al. [35] presented the bending analysis of functionally graded porous beams using the PNS concept and Timoshenko beam theory. Derikvand [36] investigated the buckling behavior of a sandwich beam that had face layers made of functionally graded materials and a porous ceramic core. Van Vinh et al. [37] introduced a static bending analysis of the FGP by developing an improved first-order beam element that considers the PNS position.

While some previous studies investigated the buckling analysis of FGBs using the PNS position concept, these have primarily focused on thermal buckling and thermal post-buckling analysis [38] and [31]. To the best of the author's knowledge, no studies have yet presented a comprehensive investigation of arbitrary boundary conditions for critical buckling loads value of FGB using the neutral surface position concept. This gap in the literature emphasizes the need for further research. The current paper fills this gap by presenting a novel and comprehensive study on the buckling analysis of the FG Timoshenko beam with arbitrary boundary conditions, all based on the PNS position concept. The study investigates the variations of critical buckling load value of the FG Timoshenko beam in relation to the slenderness ratio,

value of the power law index, and boundary conditions.

2. Material and Method

In this study, we consider a FG beam of length L , width b , and thickness h .

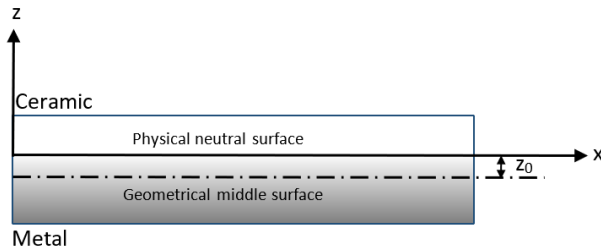


Figure 1. Position of the physical neutral surface.

The rule of mixture is utilized for defining effective properties of functionally graded beam.

$$E(z) = E_m + (E_c - E_m) \left(z + \frac{h}{2}\right)^k \quad (1)$$

$$\rho(z) = \rho_m + (\rho_c - \rho_m) \left(z + \frac{h}{2}\right)^k \quad (2)$$

where k is denotes for the power law index, E and ρ is the elasticity modulus and the density of functionally graded beam, respectively. Subscript c for ceramic and m for metal.

$$U = \int_0^L \int_{-\frac{h}{2}}^{\frac{h}{2}} (\sigma_x \varepsilon_x + \tau_{xz} \gamma_{xz}) dz dx = \int_0^L \left(A_{11} \left(\frac{\partial u}{\partial x}\right)^2 + 2B_{11} \frac{\partial \varphi}{\partial x} \frac{\partial u}{\partial x} + D_{11} \left(\frac{\partial \varphi}{\partial x}\right)^2 + A_{55} \varphi^2 + 2A_{55} \varphi \frac{\partial w}{\partial x} + A_{55} \left(\frac{\partial w}{\partial x}\right)^2 \right) dx \quad (12)$$

Total potential energy due to the external axial load (P_0) can be written as follows:

$$V = \int_0^L \frac{1}{2} P_0 \left(\frac{\partial w}{\partial x}\right)^2 dx \quad (13)$$

$$\Pi = \int_0^L \left(A_{11} \left(\frac{\partial u}{\partial x}\right)^2 + 2B_{11} \frac{\partial \varphi}{\partial x} \frac{\partial u}{\partial x} + D_{11} \left(\frac{\partial \varphi}{\partial x}\right)^2 + A_{55} \varphi^2 + 2A_{55} \varphi \frac{\partial w}{\partial x} + A_{55} \left(\frac{\partial w}{\partial x}\right)^2 \right) dx - \int_0^L \frac{1}{2} P_0 \left(\frac{\partial w}{\partial x}\right)^2 dx \quad (15)$$

The rigidities are given as follows:

$$\{A_{11}, B_{11}, D_{11}\} = \int_{-\frac{h}{2}}^{\frac{h}{2}} \{1, (z - z_0), (z - z_0)^2\} Q_{11} dz \quad (16)$$

$$A_{55} = \int_{-\frac{h}{2}}^{\frac{h}{2}} K_s Q_{55} dz \quad (17)$$

Shear correction factor K_s is taken as 5/6.

For the solution of the governing equations Ritz method is employed. Displacement function u , w , φ is defined as follows:

$$u(x) = \sum_{i=1}^n c_i f_u \quad (18)$$

In this study reference surface of the FGB assume as the PNS (Fig.1) and the coordinates of axis is defined as follows [15]:

$$z_0 = \frac{\int_{-\frac{h}{2}}^{\frac{h}{2}} z E(z) dz}{\int_{-\frac{h}{2}}^{\frac{h}{2}} E(z) dz} = \frac{\int_{-\frac{h}{2}}^{\frac{h}{2}} z \left(E_m + (E_c - E_m) \left(z + \frac{h}{2}\right)^k \right) dz}{\int_{-\frac{h}{2}}^{\frac{h}{2}} \left(E_m + (E_c - E_m) \left(z + \frac{h}{2}\right)^k \right) dz} \quad (3)$$

The displacement field is defined for the functionally graded Timoshenko beam as follows:

$$u = u_0(x) - (z - z_0) \varphi_x(x) \quad (4)$$

$$w = w(x) \quad (5)$$

Strain-displacement relations are written as:

$$\varepsilon_x = \frac{\partial u_0}{\partial x} - (z - z_0) \frac{\partial \varphi}{\partial x} \quad (6)$$

$$\gamma_{xz} = \frac{dw_0}{dx} + \varphi \quad (7)$$

Constitutive relations can be derived as follows:

$$\sigma_x = Q_{11}(z) \varepsilon_x \quad (8)$$

$$\tau_{xz} = Q_{55}(z) \gamma_{xz} \quad (9)$$

where

$$Q_{11}(z) = E(z) \quad (10)$$

$$Q_{55}(z) = \frac{E(z)}{2(1+\nu)} \quad (11)$$

The strain energy of functionally graded beam can be given as:

Total potential energy can be derived by:

$$\Pi = U - V \quad (14)$$

Table 1. Trivial functions for boundary conditions

	S-S	C-C	C-S	C-F
f_u	x^i	$x^i(L-x)$	$x^i(L-x)$	x^i
f_w	$x^i(L-x)$	$x^i(L-x)$	$x^i(L-x)$	x^{i+1}
f_φ	x^{i-1}	$x^i(L-x)$	x^i	x^i

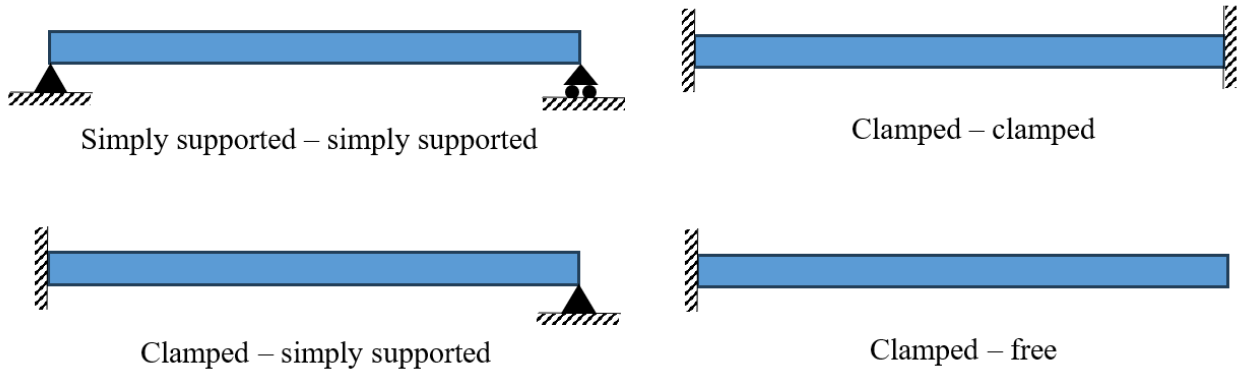


Figure 2. Boundary conditions of FG beam

For the buckling analysis, the governing equations can be obtained by substituting Eqs. (18-20) into Eq. (15) then minimizing the total energy function with respect to c_i, d_i, e_i

$$\frac{\partial \Pi}{\partial c_i} = 0 \tag{21}$$

$$\frac{\partial \Pi}{\partial d_i} = 0 \tag{22}$$

$$\frac{\partial \Pi}{\partial e_i} = 0 \tag{23}$$

The buckling behavior of functionally graded beam can be obtained by:

$$\left(\begin{bmatrix} [K_{11}] & 0 & [K_{13}] \\ 0 & [K_{22}] & [K_{32}] \\ [K_{13}] & [K_{23}] & [K_{33}] \end{bmatrix} - P_0 \begin{bmatrix} 0 & 0 & 0 \\ 0 & [K_G] & 0 \\ 0 & 0 & 0 \end{bmatrix} \right) \begin{Bmatrix} \{c\} \\ \{d\} \\ \{e\} \end{Bmatrix} = 0 \tag{24}$$

where $\{\{c\}, \{d\}, \{e\}\}^T$ is vector of unknown coefficients. Stiffness matrix $[K_{mn}]$ can be obtained as follows:

$$K_{11}(i, j) = \sum_{i=1}^n \sum_{j=1}^n \int_{-\frac{h}{2}}^{\frac{h}{2}} A_{11} \frac{df_{u_i}}{dx} \frac{df_{u_j}}{dx} dx \tag{25}$$

$$K_{13}(i, j) = - \sum_{i=1}^n \sum_{j=1}^n \int_{-\frac{h}{2}}^{\frac{h}{2}} B_{11} \frac{df_{u_i}}{dx} \frac{df_{\varphi_j}}{dx} dx \tag{26}$$

$$K_{22}(i, j) = \sum_{i=1}^n \sum_{j=1}^n \int_{-\frac{h}{2}}^{\frac{h}{2}} K_s A_{55} \frac{df_{w_i}}{dx} \frac{df_{w_j}}{dx} dx \tag{27}$$

$$K_{23}(i, j) = - \sum_{i=1}^n \sum_{j=1}^n \int_{-\frac{h}{2}}^{\frac{h}{2}} K_s A_{55} \frac{df_{w_i}}{dx} f_{\varphi_j} dx \tag{28}$$

$$K_{31}(i, j) = - \sum_{i=1}^n \sum_{j=1}^n \int_{-\frac{h}{2}}^{\frac{h}{2}} B_{11} \frac{df_{\varphi_j}}{dx} \frac{df_{u_i}}{dx} dx \tag{29}$$

$$K_{32}(i, j) = - \sum_{i=1}^n \sum_{j=1}^n \int_{-\frac{h}{2}}^{\frac{h}{2}} K_s A_{55} f_{\varphi_i} \frac{df_{w_j}}{dx} dx \tag{30}$$

$$K_{33}(i, j) = \sum_{i=1}^n \sum_{j=1}^n \int_{-\frac{h}{2}}^{\frac{h}{2}} D_{11} \frac{df_{\varphi_i}}{dx} \frac{df_{\varphi_j}}{dx} dx + \sum_{i=1}^n \sum_{j=1}^n \int_{-\frac{h}{2}}^{\frac{h}{2}} K_s A_{55} f_{\varphi_i} f_{\varphi_j} dx \tag{31}$$

$$K_G(i, j) = \sum_{i=1}^n \sum_{j=1}^n \int_{-\frac{h}{2}}^{\frac{h}{2}} \frac{df_{w_i}}{dx} \frac{df_{w_j}}{dx} dx \tag{32}$$

Critical buckling load can be found from the homogenous equation system as its lowest eigenvalue.

3. Results and Discussion

The investigation focused on analyzing the buckling behavior of functionally graded Timoshenko beams with arbitrary boundary conditions. The analysis centered on examining critical buckling loads in relation to factors such as slenderness ratio, boundary conditions, and the power-law index. This section presents the numerical results of the buckling analysis of the functionally graded Timoshenko beam. Effective properties of metal and ceramic are selected as $E_m=70\text{GPa}$, $E_c=380\text{GPa}$. Poisson's ratio is taken constant and is assumed as $\nu=0.3$, unless specifically stated otherwise. For convenience, the non-dimensional parameter is used for the critical buckling load:

$$P_{cr} = P_0 \frac{12L^2}{E_m h^3}$$

Utilizing the rule of mixture, the effective properties of the FG beam were defined. Notably, the physical neutral surface was assumed as a reference surface, simplifying the analysis. The numerical results portrayed the variation of the non-dimensional neutral surface position with the power law index for different material property ratios. It was observed that as the power law index increased, the divergence of the neutral surface from the geometrical centroidal axis decreased, indicating a convergence towards isotropic behavior. Figure 3 shows the variation of the non-dimensional neutral surface position (NSP) concerning the power-law index for different elasticity modulus ratios. As known, the position of the neutral surface coincides with the geometrical centroidal axis for isotropic material. In functionally graded material, on the other hand, this position diverges from the geometrical centroidal axis as material properties become distinct. As shown in the figure, this divergence increases as the E_c/E_m ratio increases. The non-dimensional coordinates of the neutral surface increases with power law index (k) to specific values for each ratio. After passing this index value, z_0/h decreases as the power law index value increases. This is because the metallic properties increase as the k value increases in other words, the material properties of the beam approach isotropic.

Table 2 and Table 3 show the non-dimensional critical buckling load value of FG Timoshenko beam for arbitrary boundary conditions. To verify the solution, Table 2 compares the current results with those of [13] and [16] based on FOSDT, [8] based on refined shear deformation theory

(RSdT). Similarly, Table 3 compares current results with [17] based on Timoshenko (TB) and Levinson (LB) beams. The results are in good agreement with the reference results. Comparative analysis with existing literature showed consistency and alignment with prior research findings. The agreement between the current results and reference values validated the strength of the analytical approach used in this study. The results show that the closest values are obtained for the CF beam, while the values for the SS and CC beams are slightly different from the reference values. The reason for this might be the change in the shear effect with the boundary conditions. As power law index value increases, the non-dimensional critical buckling load value decreases due to the increase in the metallic properties of the functionally graded beam. As L/h ratio decreases, the critical buckling load value decreases as the flexibility of the beam decreases. The critical buckling load values were significantly influenced by the boundary conditions. Beams with clamped-free (CF) boundary conditions displayed the highest critical load values, while those with simply supported (SS) or clamped-clamped (CC) boundary conditions showed comparatively lower values. This difference can be attributed to the varying degrees of restraint imposed by different boundary conditions, which impact the overall stability of the beam.

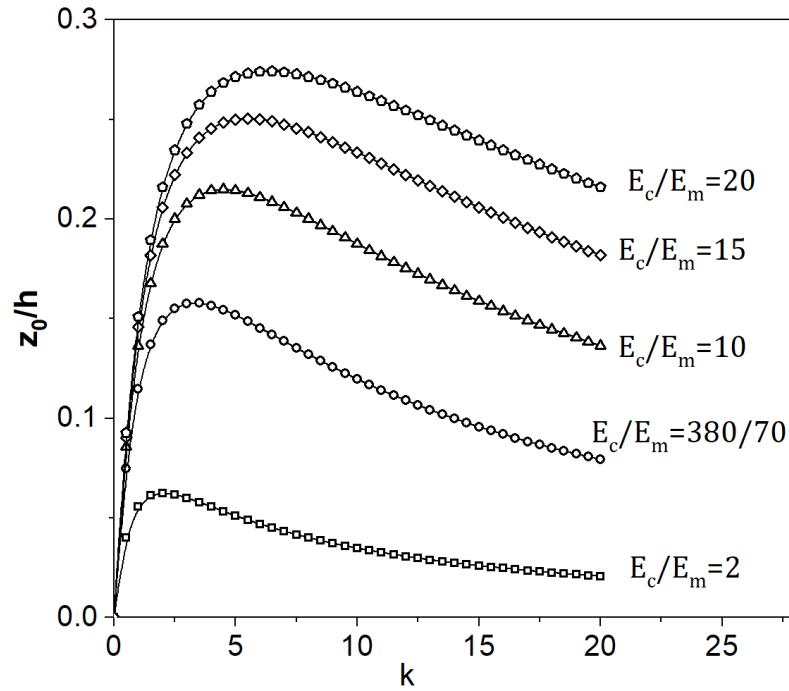


Figure 3. Variation of non-dimensional coordinates of neutral surface (z_0/h) with the power law index (k) for various E_c/E_m ratios

Table 2. Non-dimensional critical buckling load of functionally graded beam

L/h	B.C.	Ref.	k=0	k=0.5	k=1	k=2	k=5	k=10
5	CC	[13]	154.3500	103.2200	80.4980	62.6140	50.3840	44.2670
		[8]	154.4150	103.2750	80.5480	62.6616	50.4207	44.2946
		Present	151.9319	102.7112	79.3843	61.7402	49.5793	43.4983
	SS	[13]	48.8350	31.9670	24.6870	19.2450	16.0240	14.4270
		[16]	48.8350	31.9610	24.6870	19.2450	16.0240	14.4270
		[8]	48.8372	31.9695	24.6898	19.2479	16.0263	14.4286
	Present		48.5904	31.8231	24.5844	19.1616	15.9417	14.3465
	CF	[13]	13.2130	8.5782	6.6002	5.1495	4.3445	3.9501
		[8]	13.0770	8.4992	6.5428	5.1042	4.2986	3.9031
Present		13.0670	8.4900	6.5371	5.1000	4.2943	3.8979	
CS	Present	89.0643	58.9453	45.7487	35.6236	29.1454	25.9088	
10	CC	[13]	195.3400	127.8700	98.7490	76.9800	64.0960	57.7080
		[8]	195.3730	127.9050	98.7923	77.0261	64.1324	57.7329
		Present	194.3623	127.2926	98.3263	76.6474	63.7669	57.3778
	SS	[13]	52.3090	33.9960	26.1710	20.4160	17.1920	15.6120
		[16]	52.3080	33.9890	26.1710	20.4160	17.1940	15.6120
		[8]	52.3085	33.9981	26.1728	20.4187	17.1959	15.6134
	Present		52.2857	33.9566	26.1429	20.3931	17.1771	15.5880
	CF	[13]	13.2130	8.5666	6.6570	5.1944	4.3903	3.9969
		[8]	13.3137	8.6363	6.6425	5.1830	4.3785	3.9850
Present		13.3097	8.6337	6.6406	5.1823	4.3783	3.9840	
CS	Present	103.6303	67.5806	52.1023	40.6320	34.0357	30.7791	
20	CC	Present	208.9496	135.8224	104.5632	81.5712	68.6805	62.3520
	SS	Present	53.2364	34.5342	26.5620	20.7264	17.5077	15.9383
	CF	Present	13.3731	8.6811	6.6675	5.2027	4.3984	4.0055
	CS	Present	108.0484	70.1508	53.9771	42.1128	35.5253	32.2977

Table 3. Critical buckling load of functionally graded beam (non-dimensional) ($\nu=0.23$)

h/L	BC	Ref.	0	0.1	0.5	1	2	5	10	100	10 ¹⁰
1/5	CC	[17] LB	154.35	140.36	103.41	80.329	61.783	48.333	42.162	31.010	28.433
		[17] TB	154.35	140.16	103.22	80.497	62.614	50.384	44.267	31.231	28.433
		Present	154.35	140.16	103.22	80.497	62.614	50.384	44.267	31.231	28.434
	CS	[17] LB	89.523	81.172	59.317	45.905	35.473	28.477	25.183	18.146	16.491
		[17] TB	89.971	81.476	59.491	46.152	35.941	30.883	26.206	18.338	16.573
		Present	89.971	81.477	59.491	46.152	35.942	29.449	26.207	18.339	16.574
	SS	[17] LB	48.835	44.139	31.985	24.671	19.166	15.811	14.196	9.9975	8.9959
		[17] TB	48.835	44.118	31.967	24.687	19.245	16.024	14.427	10.020	8.9959
		Present	48.835	44.118	31.967	24.687	19.245	16.024	14.427	10.020	8.9959
1/10	CC	[17] LB	195.34	176.55	127.94	98.685	76.663	64.242	56.784	39.990	35.984
		[17] TB	195.34	176.47	127.87	98.748	76.980	64.096	57.708	40.081	35.984
		Present	195.34	176.47	127.870	98.748	76.980	64.096	57.708	40.082	35.985
	CS	[17] LB	103.93	93.719	67.712	52.161	40.590	33.814	30.531	21.324	19.122
		[17] TB	103.93	93.803	67.758	52.232	40.735	34.137	30.883	21.384	19.146
		Present	103.94	93.803	67.759	52.233	40.735	34.138	30.883	21.384	19.147
	SS	[17] LB	52.308	47.180	34.002	26.166	20.394	17.132	15.544	10.778	9.6357
		[17] TB	52.308	47.174	33.996	26.170	20.416	17.194	15.612	10.784	9.6357
		Present	52.308	47.174	33.996	26.171	20.416	17.194	15.612	10.784	9.6357

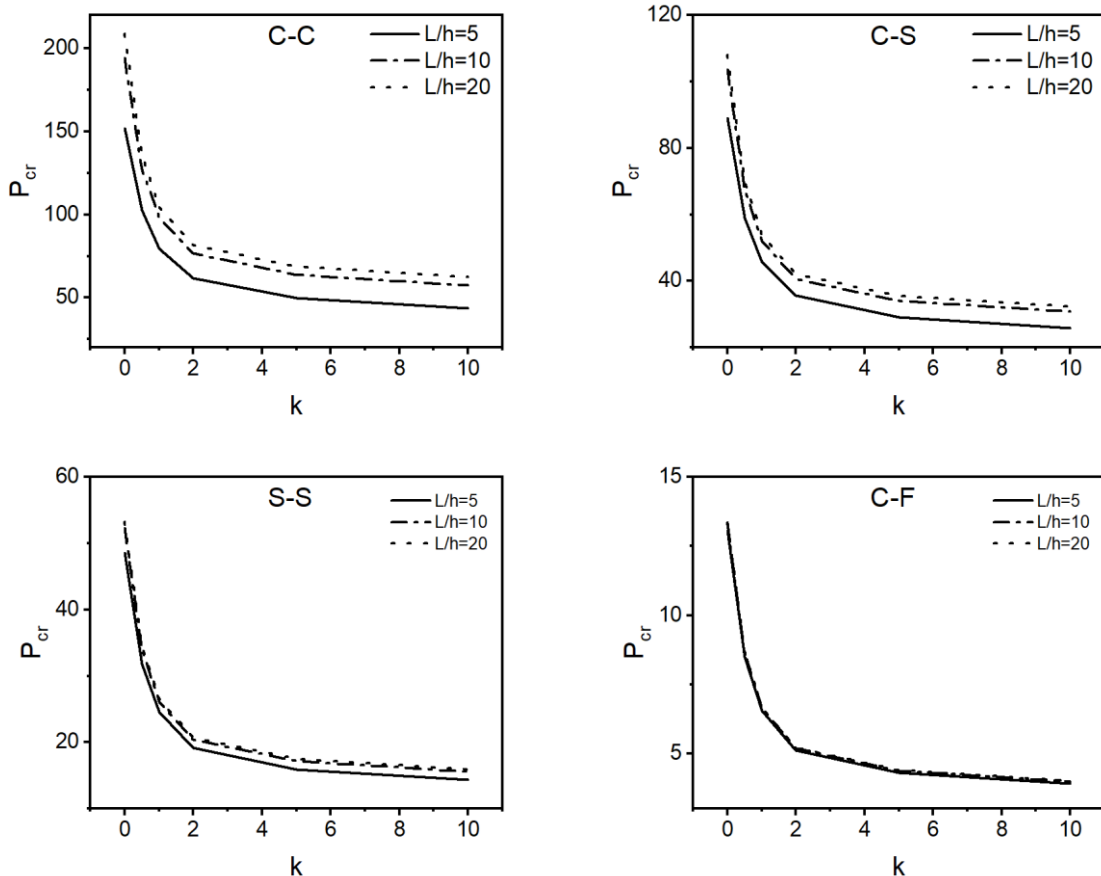


Figure 4. The non-dimensional critical buckling load for various slenderness ratio ($L/h= 5, 10, 20$)

Figure 4 illustrates the change in the critical buckling load of CC, CF, SS, and CS beams with power-law index value for various slenderness ratios ($L/h=5, 10$, and 20). As seen, the non-dimensional critical buckling load value increases with an increase

in slenderness ratio, decreases with an increase in value of power law index for all presented boundary conditions. The analysis uncovered interesting findings about how the slenderness ratio and power law index affect the critical buckling load. As the

slenderness ratio goes up, the critical load decreases, showing that higher aspect ratios lead to reduced stability. Similarly, an increase in the power law index results in lower critical buckling loads, indicating that material gradient has a diminishing effect on beam stability.

Figure 5 illustrates the non-dimensional critical buckling loads of functionally graded beam ($L/h=5, 10, \text{ and } 20$) with respect to power law index for CC, CS, SS, and CF boundary conditions. The critical load decrease with the increase in the value of power law index for all presented boundary conditions. As expected, the largest critical load values are obtained in CC beam followed by CS and SS beams, respectively. The smallest critical load values are observed in CF beam.

Figure 6 shows the non-dimensional critical buckling loads of the functionally graded beam concerning the slenderness ratio for SS, CC, CF, and

CS boundary-conditions. It is seen that the critical load value increase with the increase in slenderness ratio for all boundary conditions. The increment is more significant among the ratios 5 to 20, after passing this value, a small change is seen.

The findings highlight the complex interaction between material composition, boundary conditions, and geometric parameters in influencing the buckling behavior of functionally graded Timoshenko beams. It's important to understand these relationships for designing and optimizing structures in different engineering applications. The knowledge gained from this study offers valuable guidance for engineers and researchers aiming to improve the performance and reliability of functionally graded structures.

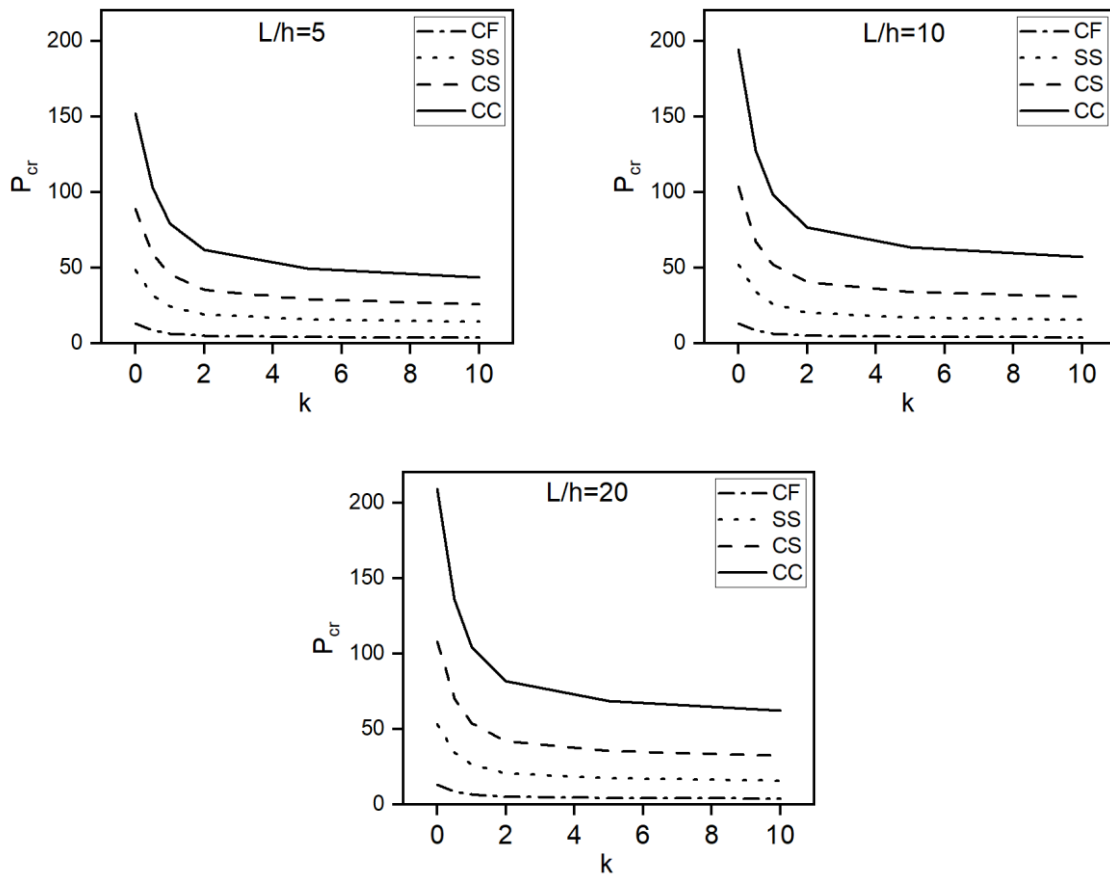


Figure 5. The non-dimensional critical buckling loads of functionally graded beam with respect to power law index for different boundary conditions

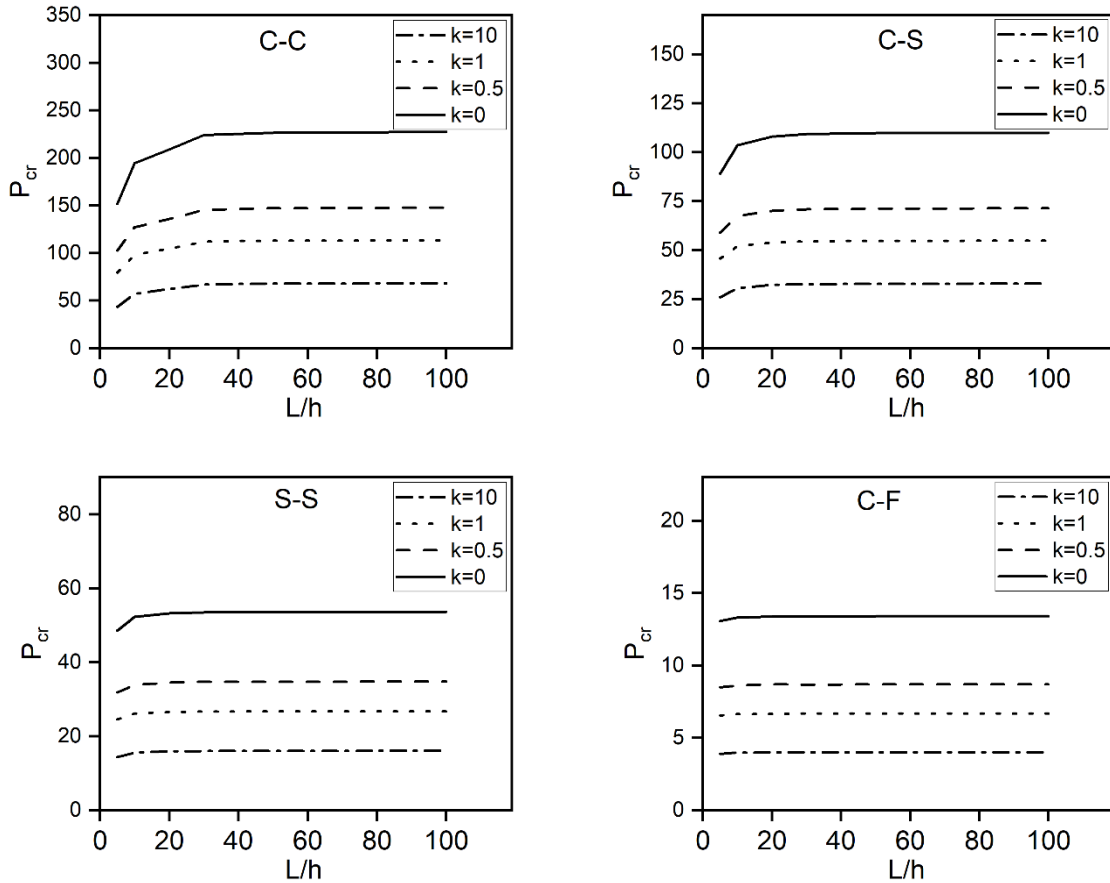


Figure 6. The non-dimensional critical buckling loads of functionally graded beam with respect to slenderness ratio for different boundary conditions

4. Conclusion and Suggestions

In this study, buckling analysis of FG Timoshenko beam is investigated. The reference surface of the FGB is assumed neutral surface then bending-stretching couplings vanished. This assumption leads to considerable simplification in the calculation. The governing equations of the FGB are derived from the principle of the minimum potential energy. The Ritz method is employed for obtaining the critical buckling load of the FGB with arbitrary boundary conditions. The current study examined the effect of boundary conditions, slenderness ratio, and power-law index value on the non-dimensional critical buckling load.

The present solution is in line with the results of previous study. The highest critical buckling load values occurred the beam with the CC boundary condition, as the CF has the lowest values. The slenderness ratio affects the critical load values adversely, the values decrease as the ratio increases. Similarly, the critical buckling loads decrease with an increase in the value of the power law index.

In conclusion, this study presents a refined understanding of the behavior of functionally graded

sandwich panels and highlights the effectiveness of advanced theoretical and computational models in predicting their responses. In particular, a novel relationship between material composition and vibration characteristics have been identified, which provides insight into the design optimization of such structures for various engineering applications.

The study may have simplified the variation of material properties, assumed certain boundary conditions and made modeling assumptions that could affect the accuracy of the predictions. It may also lack comprehensive experimental validation and have a limited scope. Acknowledging these limitations is essential for understanding the study's scope and guiding future research. A future study may be conducted to include thermal effects in addition to the presented results.

Nomenclature of Symbols and Abbreviations

L	: length of beam
B	: width
z_0	: Physical neutral surface position
ρ, ρ_m, ρ_c	: Density, density of metal, density of ceramic
E, E_m, E_c	: Elasticity modulus, Elasticity modulus of metal, Elasticity modulus of ceramic
x, y, z	: Coordinates
h	: Thickness of the beam
k	: power-law index
ν	: Poisson's ratio
u_0	: The in-plane displacements in the x direction
w_b, w_s	: Bending and shear components of the transverse displacement in the through-thickness direction
$f(z)$: The shape function
$\epsilon_x, \epsilon_z, \gamma_{xz}$: Strain components
σ_x, τ_{xz}	: Stress components
Q_{ij}	: Rigidity matrix
U	: The strain energy
V	: Potential energy
P_0	: the external axial load
K_s	: Shear correction factor
N_x, N_y, N_{xy}	: Force components
$A_{ij}, B_{ij}, B_{ij}^s, D_{ij}, D_{ij}^s, H_{ij}^s$: Rigidity matrix components
$\{K\}$: The column matrix derived from the boundary conditions of two edges parallel to the y-axis ($x=0$ and $x=a$)
u, w, φ	: Displacement function
f_u, f_w, f_φ	: Trivial functions for boundary conditions
$\{c\}, \{d\}, \{e\}^T$: vector of unknown coefficients
$[K_{mn}]$: Stiffness matrix
Π	: the total energy function
FG	: functionally graded
FGB	: functionally graded beam
FOSDT	: the first-order shear deformation beam theory
PNS	: physical neutral surface
HOSDT	: high order shear deformation theory
FGP	: functionally graded plate
BC	: boundary conditions
NSP	: neutral surface position
TB, LB	: Timoshenko and Levinson beams
CF, SS, CC, CS	: clamped-free, fully simply supported, clamped-clamped and clamped-simply supported boundary conditions

Statement of Research and Publication Ethics

The study is complied with research and publication ethics.

References

- [1] A. M. Zenkour, "A comprehensive analysis of functionally graded sandwich plates: Part 2-Buckling and free vibration," *Int J Solids Struct*, vol. 42, no. 18–19, pp. 5243–5258, Sep. 2005, doi: 10.1016/j.ijsolstr.2005.02.016.
- [2] Q. Li, V. P. Iu, and K. P. Kou, "Three-dimensional vibration analysis of functionally graded material sandwich plates," *J Sound Vib*, vol. 311, no. 1–2, pp. 498–515, Mar. 2008, doi: 10.1016/j.jsv.2007.09.018.
- [3] J. N. Reddy, *Analysis of functionally graded plates*, 2000.
- [4] T. P. Vo, H. T. Thai, T. K. Nguyen, F. Inam, and J. Lee, "A quasi-3D theory for vibration and buckling of functionally graded sandwich beams," *Compos Struct*, vol. 119, pp. 1–12, Jan. 2015, doi: 10.1016/j.compstruct.2014.08.006.
- [5] H. T. Thai and D. H. Choi, "Finite element formulation of various four unknown shear deformation theories for functionally graded plates," *Finite Elements in Analysis and Design*, vol. 75, pp. 50–61, 2013, doi: 10.1016/j.finel.2013.07.003.
- [6] V. Taskin and P. A. Demirhan, "Static analysis of simply supported porous sandwich plates," *Structural Engineering and Mechanics*, vol. 77, no. 4, pp. 549–557, Feb. 2021, doi: 10.12989/sem.2021.77.4.549.
- [7] P. A. Demirhan and V. Taskin, "Bending and free vibration analysis of Levy-type porous functionally graded plate using state space approach," *Compos B Eng*, vol. 160, pp. 661–676, Mar. 2019, doi: 10.1016/j.compositesb.2018.12.020.
- [8] T. P. Vo, H. T. Thai, T. K. Nguyen, A. Maheri, and J. Lee, "Finite element model for vibration and buckling of functionally graded sandwich beams based on a refined shear deformation theory," *Eng Struct*, vol. 64, pp. 12–22, Apr. 2014, doi: 10.1016/j.engstruct.2014.01.029.
- [9] C. P. Sreeju Nair S B, "Functionally Graded Panels: A Review," *International Journal for Modern Trends in Science and Technology*, no. 8, pp. 36–43, Aug. 2020, doi: 10.46501/ijmtst060808.
- [10] C. Pany and G. V. Rao, "Calculation of non-linear fundamental frequency of a cantilever beam using non-linear stiffness," *Journal of Sound and Vibration*, vol. 256, no. 4. Academic Press, pp. 787–790, Sep. 26, 2002. doi: 10.1006/jsvi.2001.4224.
- [11] C. Pany and G. V. Rao, "Large amplitude free vibrations of a uniform spring-hinged beam," *J Sound Vib*, vol. 271, no. 3–5, pp. 1163–1169, Apr. 2004, doi: 10.1016/S0022-460X(03)00572-8.
- [12] C. Pany, "Large amplitude free vibrations analysis of prismatic and non-prismatic different tapered cantilever beams," *Pamukkale University Journal of Engineering Sciences*, vol. 29, no. 4, pp. 370–376, 2023, doi: 10.5505/pajes.2022.02489.
- [13] S. R. Li and R. C. Batra, "Relations between buckling loads of functionally graded timoshenko and homogeneous euler-bernoulli beams," *Compos Struct*, vol. 95, pp. 5–9, Jan. 2013, doi: 10.1016/j.compstruct.2012.07.027.
- [14] S. R. Li, D. F. Cao, and Z. Q. Wan, "Bending solutions of FGM Timoshenko beams from those of the homogenous Euler-Bernoulli beams," *Appl Math Model*, vol. 37, no. 10–11, pp. 7077–7085, Jun. 2013, doi: 10.1016/j.apm.2013.02.047.
- [15] V. L. Nguyen, M. T. Tran, V. L. Nguyen, and Q. H. Le, "Static behaviour of functionally graded plates resting on elastic foundations using neutral surface concept," *Archive of Mechanical Engineering*, vol. 68, no. 1, pp. 5–22, 2021, doi: 10.24425/ame.2020.131706.
- [16] T. K. Nguyen, T. P. Vo, and H. T. Thai, "Static and free vibration of axially loaded functionally graded beams based on the first-order shear deformation theory," *Compos B Eng*, vol. 55, pp. 147–157, 2013, doi: 10.1016/j.compositesb.2013.06.011.
- [17] S. Li, X. Wang, and Z. Wan, "Classical and homogenized expressions for buckling solutions of functionally graded material Levinson beams," *Acta Mechanica Solida Sinica*, vol. 28, no. 5, pp. 592–604, Oct. 2015, doi: 10.1016/S0894-9166(15)30052-5.
- [18] T. Morimoto, Y. Tanigawa, and R. Kawamura, "Thermal buckling of functionally graded rectangular plates subjected to partial heating," *Int J Mech Sci*, vol. 48, no. 9, pp. 926–937, Sep. 2006, doi: 10.1016/j.ijmecsci.2006.03.015.
- [19] S. Abrate, "Functionally graded plates behave like homogeneous plates," *Compos B Eng*, vol. 39, no. 1, pp. 151–158, Jan. 2008, doi: 10.1016/j.compositesb.2007.02.026.

- [20] D. G. Zhang and Y. H. Zhou, "A theoretical analysis of FGM thin plates based on physical neutral surface," *Comput Mater Sci*, vol. 44, no. 2, pp. 716–720, Dec. 2008, doi: 10.1016/j.commatsci.2008.05.016.
- [21] D. G. Zhang, "Modeling and analysis of FGM rectangular plates based on physical neutral surface and high order shear deformation theory," *Int J Mech Sci*, vol. 68, pp. 92–104, Mar. 2013, doi: 10.1016/j.ijmecsci.2013.01.002.
- [22] A. Fekrar, M. S. A. Houari, A. Tounsi, and S. R. Mahmoud, "A new five-unknown refined theory based on neutral surface position for bending analysis of exponential graded plates," *Meccanica*, vol. 49, no. 4, pp. 795–810, 2014, doi: 10.1007/s11012-013-9827-3.
- [23] D. G. Zhang, "Nonlinear bending analysis of FGM rectangular plates with various supported boundaries resting on two-parameter elastic foundations," *Archive of Applied Mechanics*, vol. 84, no. 1, pp. 1–20, Jan. 2014, doi: 10.1007/s00419-013-0775-0.
- [24] S. C. Han, W. T. Park, and W. Y. Jung, "A four-variable refined plate theory for dynamic stability analysis of S-FGM plates based on physical neutral surface," *Compos Struct*, vol. 131, pp. 1081–1089, Nov. 2015, doi: 10.1016/j.compstruct.2015.06.025.
- [25] H. Bellifa, K. H. Benrahou, L. Hadji, M. S. A. Houari, and A. Tounsi, "Bending and free vibration analysis of functionally graded plates using a simple shear deformation theory and the concept the neutral surface position," *Journal of the Brazilian Society of Mechanical Sciences and Engineering*, vol. 38, no. 1, pp. 265–275, Jan. 2016, doi: 10.1007/s40430-015-0354-0.
- [26] F. Ebrahimi, A. Jafari, and M. R. Barati, "Free Vibration Analysis of Smart Porous Plates Subjected to Various Physical Fields Considering Neutral Surface Position," *Arab J Sci Eng*, vol. 42, no. 5, pp. 1865–1881, May 2017, doi: 10.1007/s13369-016-2348-3.
- [27] V. L. Nguyen, M. T. Tran, V. L. Nguyen, and Q. H. Le, "Static behaviour of functionally graded plates resting on elastic foundations using neutral surface concept," *Archive of Mechanical Engineering*, vol. 68, no. 1, pp. 5–22, 2021, doi: 10.24425/ame.2020.131706.
- [28] A. Sadgui and A. Tati, "A novel trigonometric shear deformation theory for the buckling and free vibration analysis of functionally graded plates," *Mechanics of Advanced Materials and Structures*, vol. 29, no. 27 pp. 6648-6663, 2021, doi: 10.1080/15376494.2021.1983679.
- [29] L. S. Ma and D. W. Lee, "Exact solutions for nonlinear static responses of a shear deformable FGM beam under an in-plane thermal loading," *European Journal of Mechanics, A/Solids*, vol. 31, no. 1, pp. 13–20, Jan. 2012, doi: 10.1016/j.euromechsol.2011.06.016.
- [30] L. O. Larbi, A. Kaci, M. S. A. Houari, and A. Tounsi, "An efficient shear deformation beam theory based on neutral surface position for bending and free vibration of functionally graded beams," *Mechanics Based Design of Structures and Machines*, vol. 41, no. 4, pp. 421–433, Oct. 2013, doi: 10.1080/15397734.2013.763713.
- [31] D. G. Zhang, "Thermal post-buckling and nonlinear vibration analysis of FGM beams based on physical neutral surface and high order shear deformation theory," *Meccanica*, vol. 49, no. 2, pp. 283–293, Feb. 2014, doi: 10.1007/s11012-013-9793-9.
- [32] K. S. Al-Basyouni, A. Tounsi, and S. R. Mahmoud, "Size dependent bending and vibration analysis of functionally graded micro beams based on modified couple stress theory and neutral surface position," *Compos Struct*, vol. 125, pp. 621–630, Jul. 2015, doi: 10.1016/j.compstruct.2014.12.070.
- [33] F. Ebrahimi and E. Salari, "A Semi-analytical Method for Vibrational and Buckling Analysis of Functionally Graded Nanobeams Considering the Physical Neutral Axis Position," 2015.
- [34] K. Zoubida, T. H. Daouadji, L. Hadji, A. Tounsi, and A. B. el Abbas, "A New Higher Order Shear Deformation Model of Functionally Graded Beams Based on Neutral Surface Position," *Transactions of the Indian Institute of Metals*, vol. 69, no. 3, pp. 683–691, Apr. 2016, doi: 10.1007/s12666-015-0540-x.
- [35] N. T. B. Phuong, T. M. Tu, H. T. Phuong, and N. van Long, "Bending analysis of functionally graded beam with porosities resting on elastic foundation based on neutral surface position," *Journal of Science and Technology in Civil Engineering (STCE) - NUCE*, vol. 13, no. 1, pp. 33–45, Jan. 2019, doi: 10.31814/stce.nuce2019-13(1)-04.
- [36] M. Derikvand, F. Farhatnia, and D. H. Hodges, "Functionally graded thick sandwich beams with porous core: Buckling analysis via differential transform method," *Mechanics Based Design of Structures and Machines*, vol. 51, no. 7, pp. 3650-3677, 2021, doi: 10.1080/15397734.2021.1931309.

- [37] P. Van Vinh, N. Q. Duoc, and N. D. Phuong, "A New Enhanced First-Order Beam Element Based on Neutral Surface Position for Bending Analysis of Functionally Graded Porous Beams," *Iranian Journal of Science and Technology - Transactions of Mechanical Engineering*, vol. 46, no. 4, pp. 1141–1156, Dec. 2022, doi: 10.1007/s40997-022-00485-1.
- [38] Y. Liu, S. Su, H. Huang, and Y. Liang, "Thermal-mechanical coupling buckling analysis of porous functionally graded sandwich beams based on physical neutral plane," *Compos B Eng*, vol. 168, pp. 236–242, Jul. 2019, doi: 10.1016/j.compositesb.2018.12.063.